ELSEVIER

Toxicon 50 (2007) 330–338

TOXICON

www.elsevier.com/locate/toxicon

Effects of microcystin-LR on mouse lungs

Raquel M. Soares[a,*], Viviane R. Cagido[b], Rodrigo B. Ferraro[c], José Roberto Meyer-Fernandes[c], Patrícia R.M. Rocco[d], Walter A. Zin[b], Sandra M.F.O. Azevedo[a]

[a]*Laboratory of Ecophysiology and Toxicology of Cyanobacteria, Carlos Chagas Filho Institute of Biophysics, Federal University of Rio de Janeiro, CCS, BL-G, llha do Fundão, 21949-900 Rio de Janeiro, Brazil*

[b]*Laboratory of Respiration Physiology, Carlos Chagas Filho Institute of Biophysics, Federal University of Rio de Janeiro, CCS, BL-G, llha do Fundão, 21949-900 Rio de Janeiro, Brazil*

[c]*Laboratory of Cellular Biochemistry, Institute of Medical Biochemistry, Federal University of Rio de Janeiro, CCS, BL-H, llha do Fundão, 21949-900 Rio de Janeiro, Brazil*

[d]*Laboratory of Pulmonary Investigation, Carlos Chagas Filho Institute of Biophysics, Federal University of Rio de Janeiro, CCS, BL-G, llha do Fundão, 21949-900 Rio de Janeiro, Brazil*

Received 14 February 2007; received in revised form 30 March 2007; accepted 2 April 2007
Available online 11 April 2007

Abstract

Toxic cyanobacteria blooms in drinking water supplies have been an increasing public health concern all over the world. Human populations can be exposed to microcystins, an important family of cyanotoxins, mainly by oral ingestion. However, inhalation from recreational water and hemodialysis can represent other routes. This study investigated changes in respiratory mechanics, histology, protein phosphatase (PP) 1 and 2A activity and microcystin in lung of adult mice injected intraperitoneally (i.p.) with microcystin-LR. Thirty-six mice were divided into control (CTRL) and test (CYANO) groups. CTRL group received an i.p. injection of saline and the CYANO group received 40 μg MCYST-LR/kg i.p. After 2 and 8 h, and 1, 2 and 4 days after toxin injection, six mice from each group were sampled for analyses. Resistive and viscoelastic pressures, static and dynamic elastances augmented at 2 h in CYANO and so remained until day 4. Alveolar collapse and inflammatory cell infiltration were found 2 h after the injection, reaching peak values at 8 h. However, no microcystin or inhibition of PPases could be detected in mice lungs. In conclusion, MCYST-LR led to a rapid increase in lung impedance and an inflammatory response with interstitial edema and inflammatory cell recruitment in mice.

Keywords: Microcystin-LR; Lung; Inflammation; Alveolar collapse

1. Introduction

In the last decade, public health concern about cyanobacteria and cyanotoxins has increased in many countries, owing to their frequent occurrence in aquatic ecosystems used for different purposes, including those used as drinking water supplies. Microcystins are the cyanotoxins most frequently found all over the world. Their toxic effects have been described in organisms as diverse as macrophytes, zooplankton, fish and mammals (Francis, 1878; Sahin et al., 1995; Ferrão-Filho and Azevedo, 2002; Pflugmacher, 2002).

*Corresponding author.
E-mail address: rmsoares@biof.ufrj.br (R.M. Soares).

0041-0101/$ - see front matter © 2007 Elsevier Ltd. All rights reserved.
doi:10.1016/j.toxicon.2007.04.003

Microcystins are cyclic heptapeptides, containing five D-amino acids and two variable L-amino acids. So far, more than 70 microcystin variants have been characterized (Chorus and Bartram, 1999). In vertebrate animals, the main targets of microcystins are the hepatic cells, where they irreversibly inhibit protein phosphatases (PP) of the serine/threonine family, especially PP1 and PP2A. Acutely, this effect causes cytoskeleton disarrangement of hepatocytes, which leads to hepatic failure. Chronically, sub-lethal doses of microcystins can promote tumors in tissues such as skin, colon and liver (Falconer et al., 1988; Humpage et al., 2000).

The first confirmed report of human deaths related to microcystins intoxication occurred in Brazil in 1996, when more than 70 renal patients died after hemodialysis treatment using water contaminated with microcystins (Jochimsen et al., 1998; Carmichael et al., 2001; Azevedo et al., 2002). More recently, another case of human exposure to these cyanotoxins occurred in Brazil despite the efforts of the public health authorities, including new legislation that considers microcystins as a mandatory parameter to be monitored in drinking water. Hemodialysis patients in Rio de Janeiro were exposed to sub-lethal doses of microcystins, and fortunately, no symptoms of hepatic damage were observed (Soares et al., 2006).

Efforts to understand the sub-lethal toxicological effects of microcystins have become important since human populations are exposed more frequently to low doses of microcystins than to lethal ones. Furthermore, it is known that in addition to hepatic function effects, damage to renal function and to the gastrointestinal mucosa has been described in the literature (Nobre et al., 2001; Moreno et al., 2003; Botha et al., 2004). The respiratory system can also be compromised, but more information about this aggression is still needed.

Turner et al. (1990) reported a case of two recruits in England who developed severe pneumonia after contact with water containing toxic *Microcystis aeruginosa*, and Slatkin et al. (1983) detected pulmonary thrombosis in mice intraperitoneally (i.p.) injected with lethal doses of microcystins. It has been already demonstrated that this toxin can reach the lung, and its distribution after oral and intratracheal administrations has been well described by Ito et al. (2000, 2001).

Recently, we have reported a rapid and continued inflammatory process with interstitial edema and recruitment of inflammatory cells, plus alveolar collapse, in the lungs of Swiss mice injected with a sub-lethal i.p. dose of an aqueous extract obtained from a toxic *M. aeruginosa* strain (Picanço et al., 2004). Thus, the aim of this study is to validate and expand the aforementioned results as a result of the administration of a sub-lethal dose of purified microcystin-LR (MCYST-LR). For such purpose the activity of protein phosphatase, the histological and mechanical profiles were measured in the lungs of Swiss mice.

2. Material and methods

2.1. Animal preparation

The experiments were done on normal adult male Swiss mice weighing from 25 to 30 g and aging 6–8 weeks obtained from the Oswaldo Cruz Institute, Rio de Janeiro. Thirty-six animals were randomly divided into two groups: control animals (CTRL, $n = 6$) were i.p. injected with 300 μL of saline (0.9% NaCl) and test animals (CYANO, $n = 30$) received a sub-lethal dose of MCYST-LR (40 μg/kg i.p., purified material kindly provided by Professor Wayne Carmichael, Wright State University, USA). Respiratory mechanics, lung histology, protein phosphatases activity and enzyme-linked immunosorbent assay (ELISA) analyses were done at 2 and 8 h, and, 1, 2 and 4 days after MCYST-LR i.p. administration. The control animals were randomly sampled during the 96 h of the experiment.

This study was approved by the Ethics Committee of the Carlos Chagas Filho Institute of Biophysics, Health Sciences Center, Federal University of Rio de Janeiro. All animals received humane care in compliance with the "Principles of Laboratory Animal Care" formulated by the National Society for Medical Research and the "Guide for the Care and Use of Laboratory Animals" prepared by the National Academy of Sciences, USA.

2.2. Experimental protocol

The animals of both groups were sedated with diazepam (1 mg/kg i.p.) and anesthetized with pentobarbital sodium (20 mg/kg i.p.). The animals were placed in the supine position on a surgical table and a snugly fitting cannula (0.5 mm i.d.) was introduced into the trachea. Muscle relaxation was achieved with pancuronium bromide (0.4 mg/kg i.v.) and artificial ventilation was provided by a constant

flow ventilator (Samay VR15, Universidad de la Republica, Montevideo, Uruguay) with a frequency of 100 breaths/min. During the test breaths, the ventilator was adjusted to generate a 5-s end-inspiratory pause, whereas no pause was used during baseline ventilation. Special care was taken to keep tidal volume ($V_T = 0.2$ ml) and flow ($V' = 1$ ml/s) constant in all animals in order to avoid the effects of different flows, volumes (Kochi et al., 1988) and inspiratory duration (Similowski et al., 1989) on the measured variables.

Before surgical removal of the anterior chest wall, the amount of positive end-expiratory pressure (PEEP) required to maintain functional residual capacity unaltered was determined and applied right before the pleural cavity was entered. The PEEP level was determined as follows: before the pleural space was opened, the ventilator was disconnected at end expiration, and the airways were occluded. After pleural incision, there was an increase in transpulmonary pressure (PL) that corresponded to the elastic recoil pressure of the lung at relaxation volume. Thereafter, the same pressure was applied to the lung (2 cm H_2O on the average).

A pneumotachograph (1.0 mm i.d., length = 4.2 cm, distance between side ports = 2.1 cm; Mortola and Noworaj, 1983) was connected to the tracheal cannula (0.055 mL of dead space) for measurement of airflow and changes in lung volume. The pressure gradient across the pneumotachograph was determined by means of a Validyne MP45-2 differential pressure transducer (Engineering Corp., Northridge, CA, USA). The flow resistance of the equipment (Req), tracheal cannula included, was constant up to flow rates of 26 mL/s, and amounted to 0.12 cm H_2O/mL/s. Equipment resistive pressure (= Req/V') was subtracted from pulmonary resistive pressure so that the present results represent intrinsic values. Because abrupt changes in diameter were not present in our circuit, errors of measurement of flow resistance were probably avoided. Tracheal pressure was measured with a Validyne MP-45 differential pressure transducer (Engineering Corp., Northridge, CA, USA). All signals were conditioned and amplified in a Beckman type R Dynograph (Schiller Park, IL, USA). Flow and pressure signals were then passed through eight-pole Bessel filters (902LPF, Frequency Devices, Haverhill, MA, USA) with the corner frequency set at 100 Hz, sampled at 200 Hz with a 12-bit analog-to-digital converter (DT2801A, Data Translation, Marlboro, MA, USA), and stored on a desktop computer. All data were collected using LABDAT software (RHT-InfoData Inc., Montreal, Que., Canada).

2.3. Measurement of pulmonary mechanics

Pulmonary mechanics were measured by the end-inflation occlusion method (Bates et al., 1985, 1988). In an open-chest preparation, tracheal pressure reflects PL. Briefly, after end-inspiratory occlusion, there is an initial fast drop in PL (ΔP_1) from the pre-occlusion value down to an inflection point (P_i) followed by a slow pressure decay (ΔP_2), until a plateau is reached. This plateau corresponds to the elastic recoil pressure of the lung (P_{el}). ΔP_1 selectively reflects pressure dissipated against pulmonary resistance in normal animals and humans, and ΔP_2 reflects viscoelastic properties (stress relaxation) and/or inhomogeneities of lung tissue together with a small contribution of pendelluft in normal situations (Bates et al., 1988; Similowski et al., 1989). Total pressure drop (ΔP_{tot}) is equal to the sum of ΔP_1 and ΔP_2. Lung static and dynamic elastances (E_{st} and E_{dyn}, respectively) were calculated by dividing P_{el} and P_i by V_T, respectively. ΔE was calculated as the difference $E_{dyn} - E_{st}$. Pulmonary mechanics were measured 10–15 times in each animal. All data were analyzed using ANADAT data analysis software (RHT-InfoData Inc., Montreal, Que., Canada). The duration of the experiments approximated 30 min.

2.4. Lung histology

A lower transversal laparotomy was done immediately after the determination of pulmonary mechanics, and the abdominal aorta and vena cava were sectioned, yielding a massive hemorrhage that quickly killed the animals. The trachea was clamped at end expiration and the lungs were removed *en bloc*.

Immediately afterwards, the left lung was quick frozen by immersion in liquid nitrogen and fixed with Carnoy's solution (ethanol:cloroform:acetic acid, 70:20:10 by volume) at −70 °C for 24 h. Progressively, increasing concentrations of ethanol at −20 °C substituted Carnoy's solution until 100% ethanol was reached. The tissue was maintained at −20 °C for 4 h, warmed to 4 °C for 12 h, and then allowed to reach and remain at room temperature for 2 h (Nagase et al., 1992). After fixation, the tissue was embedded in paraffin. Four-micrometer-thick tissue

slices were obtained with a microtome and stained with hematoxylin–eosin. Two investigators, who were unaware of the origin of the material, performed the histological analyses. Morphometric analysis was done with an integrating eyepiece with a coherent system made of a 100-point grid consisting of 50 lines of known length, coupled to a conventional light microscope (Axioplan, Zeiss, Oberkochen, Germany). The volume fraction of collapsed and normal pulmonary areas and the fraction of the lung occupied by large-volume gas-exchanging air spaces (hyperinflated structures with morphology distinct from that of alveoli and wider than 120 μm) were determined by the point-counting technique (Gundersen et al., 1988) at a magnification of 20 × across 10 random, non-coincident microscopic fields. Briefly, points falling on collapsed, normal or hyperinflated pulmonary areas were counted and divided by the total number of points in each microscopic field.

Polymorphonuclear (PMN) and mononuclear cells were identified according to the shape of nucleus. These cells and pulmonary tissue were evaluated by the point-counting technique (Gundersen et al., 1988) across 10 random non-coincident microscopic fields at 1000 × magnification. Points falling on the tissue area and not over air spaces were counted and divided by the total number of points in each microscopic field. Thus, data are reported as the fractional area of pulmonary tissue.

2.5. Analysis of protein phosphatases 1 and 2A activity

The right lungs of mice were homogenized for protein phosphatase activity and microcystin analyses by the method described by Runnegar et al. (1993). Briefly, the tissues were homogenized in buffer solution (0.1 g of tissue/mL) containing EDTA (0.1 mM), DTT (1 mM), Tris–HCl, pH 7.0 (50 mM) and the protease inhibitor PMSF (0.1 mM), at 4 °C, using a Tissuemiser homogenizer (Fisher Scientific, Hampton, NH, USA). The resultant homogenates were centrifuged (10,000 × *g*) and the supernatants were stored in glass vials at −20 °C until the analysis was done.

Following the procedure described by Shenolikar and Ingebritsen (1984) with minor modifications specific substrate for PP1 and 2A was produced: phosphorilase *a* [γ-^{32}P] from phosphorilase *b* and [γ-^{32}P] ATP (enzymes from Sigma-Aldrich, Saint Louis, USA; γ-^{32}ATP from Amersham Biosciences, Buckinghamshire, UK).

The phosphatase activity was determined by mixing 10 μL of homogenate supernatant, 10 μL of reaction solution (50 mM Tris–HCl, pH 7.0 and 1 mM DTT) and 10 μL of substrate solution—[γ-^{32}P] phosphorilase *a* (3 mg/mL)—during 10 min of incubation at room temperature. The reaction was stopped with 0.1 mL of 10% trichloroacetic acid. The amount of radioactive phosphate released was determined by liquid scintillation.

2.6. Microcystin analysis by ELISA

Aliquots of homogenate supernatant of the same lungs were analyzed by ELISA to investigate possible toxin accumulation in those tissues. Anti-MCYST-LR rabbit policlonal antibodies with cross reactivity against several microcystins variants were used (Chu et al., 1990; An and Carmichael, 1994; Carmichael and An, 1999). The antibodies and MCYST-horseradish peroxidase (MCYST-HRP) conjugate were kindly provided by Professor Wayne Carmichael (Wright State University, USA). Hence, 200 μL 96-well plates were incubated with rabbit polyclonal antibodies anti-MCYST LR-BSA (5 μg/mL) for 24 h (minimum) and stored at 4 °C (for up to 7 days). Prior to sample analysis, the plate was washed with buffer solution (PBS)—0.05% Tween 20 and incubated for 60 min with blocker solution (1% casein/PBS). Right after that, the plate was washed again. Then, calibrators (different concentrations of MCYST-LR—0.16–1.6 ng/mL for the standard curve) and samples were applied to their respective wells in duplicate, following an incubation time of 30 min. The MCYST-HRP (12.5 nM) conjugate was applied just after this period and the plate was incubated for another 30 min. Then, the plate was washed and received the substrate solution prepared on the spot with *o*-phenylenediamine (OPD: 0.4 mg/mL), citrate buffer (50 mM citric acid/0.1 M NaH_2PO_4, pH 5.0) and 30% H_2O_2, with 10 min of final incubation. The reaction was stopped with 1 N HCl and the absorbances were determined by a plate reader (Vmax, Molecular Devices, CA, USA) at 490 nm. The results of microcystin concentration in the samples were obtained from the MCYST-LR standard curve.

2.7. Statistical analysis

The normal distribution of the data was tested by the Kolmogorov–Smirnov test with Lilliefors' correction. Equal variances of the data were assessed

by Levene median test. If both conditions were satisfied, one-way ANOVA test was used. In the negative case, the nonparametric Kruskal–Wallis ANOVA on ranks was applied. If multiple comparisons among the treatments were then required, Tukey test was used. In all instances, the significance level was set at 5%. Statistical analyses were done with SigmaStat 2.0 statistical software package (Jandel Corporation, San Rafael, CA, USA).

3. Results

Microcystin was not detected in the lung homogenates by ELISA analysis (limit of quantification: 0.16 ppb). Additionally, the lung activity of protein phosphatases 1 and 2A remained unaltered in the CYANO group, which means that they were not inhibited by i.p. injection of MCYST-LR (Fig. 1).

However, MCYST-LR damaged the lung. Table 1 shows the values of alveolar collapse fraction in CTRL and CYANO groups. Two hours after i.p. injection of MCYST-LR, the collapse fraction increased, reaching 23.2% of the alveolar area. The percentage of PMN cells also increased significantly at 2 h after MCYST-LR i.p. injection. At this time, PMNs represented 28.8% of lung tissue. These results remained elevated throughout the 4 days of the experiment (Table 2).

Fig. 2 shows lungs from CTRL and CYANO groups, illustrating the damage to lung parenchyma. Two hours after MCYST-LR i.p. injection (panel B), a discreet edema, thickening of the alveolar septa due to PMN cells recruitment, and an increase in collapsed areas can be observed with the highest percentage at 8 h (panel C). These alterations progressively decreased without returning to the control value.

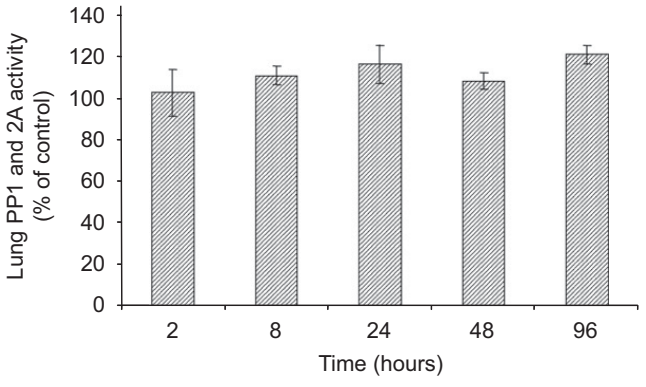

Fig. 1. Activity of protein phosphatases (PP) 1 and 2A (mU/g of tissue, expressed as percentages of control mice PP activity = 4.42 mU/g) in lungs of mice intraperitoneally injected with microcystin-LR (40 μg/kg of body weight) as a function of post-administration time. Values are means ± S.E.M. No significant differences among results at each sampling time and in relation to control could be detected at $p \leqslant 0.05$, $n = 6$).

Table 1
Percentages of normal and collapsed areas in mice lungs

Group	Normal area (%)	Alveolar collapse (%)
Control	94.7 ± 0.87^{a}	5.2 ± 0.87^{a}
2 h	$76.6 \pm 2.33^{b,c}$	$23.2 \pm 2.22^{b,c}$
8 h	70.3 ± 1.45^{b}	29.0 ± 1.17^{b}
24 h	$75.5 \pm 2.38^{b,c}$	$24.5 \pm 2.38^{b,c}$
48 h	79.4 ± 2.21^{c}	20.1 ± 2.35^{c}
96 h	81.3 ± 1.69^{c}	18.6 ± 1.69^{c}

Values are means ± S.E.M. of six adult animals (7–10 determinations in each animal) 2, 8, 24, 48 and 96 h after i.p. injection of microcystin-LR (40 μg/kg of body weight). Values marked with different superscript letters (a, b, c) are significantly different ($p < 0.05$).

Table 2
Percentages of polimorphonuclear (PMN) and mononuclear (MN) cells and the sum of both or total cells (TOT) in mice lungs in relation to the total tissue area

Group	TOT (%)	PMN (%)	MN (%)
Control	29.6 ± 1.89^{a}	9.9 ± 1.42^{a}	19.6 ± 0.95^{a}
2 h	38.0 ± 2.74^{b}	28.8 ± 2.43^{b}	9.1 ± 0.83^{b}
8 h	39.6 ± 1.79^{b}	29.0 ± 1.01^{b}	10.6 ± 1.28^{b}
24 h	37.5 ± 2.01^{b}	$25.1 \pm 2.93^{b,c}$	12.3 ± 1.63^{b}
48 h	38.9 ± 0.73^{b}	$25.7 \pm 0.55^{b,c}$	13.2 ± 0.74^{b}
96 h	33.4 ± 2.07^{a}	22.0 ± 1.34^{c}	11.4 ± 0.89^{b}

Values are means ± S.E.M. of six adult animals (7–10 determinations in each animal) 2, 8, 24, 48 and 96 h after i.p. injection of microcystin-LR (40 μg/kg of body weight). Values marked with different superscript letters (a, b, c) are significantly different ($p < 0.05$).

Pulmonary mechanical parameters revealed resistive and elastic changes in mice injected with MCYST-LR. Fig. 3 shows that at 2 h ΔP_1, ΔP_2 and ΔP_{tot} average values in CYANO group were 63%, 32% and 39% higher than in CTRL group, respectively. Statistical analyses indicated that these pulmonary mechanical parameters remained equally altered after the initial 2 h until the fourth and last sampling day. Fig. 4 shows that MCYST-LR-injected mice presented values of ΔE higher than those in the CTRL group already at 2 h post-administration of the toxin, and, furthermore, these values remained at this new level until the end of the experiment. On the other hand, static elastance was larger than CTRL at 2 h, reached its peak value at

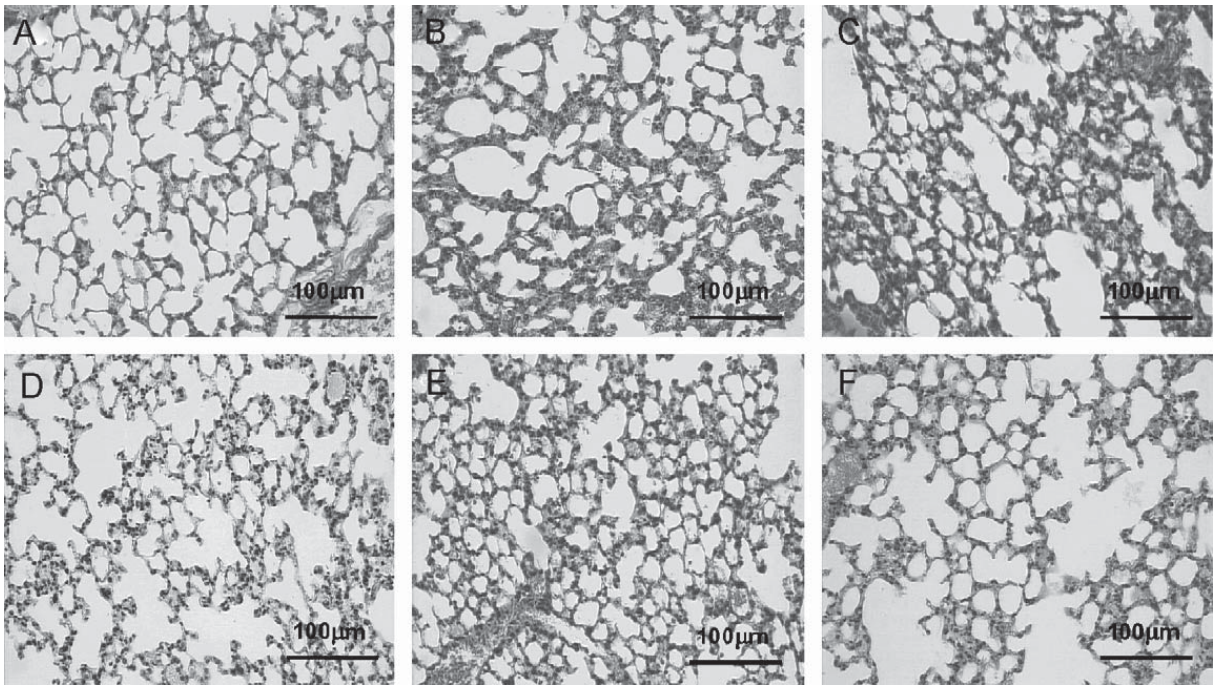

Fig. 2. Photomicrographs of lung parenchyma (200 ×). (A) Control group and (B–F) lungs gathered at 2, 8, 24, 48 and 96 h, respectively, after intraperitoneal injection of microcystin-LR (40 μg/kg of body weight).

8 h, and decreased progressively until the end of the experiment.

4. Discussion

Analysis of pulmonary mechanical parameters revealed that i.p. injection of MCYST-LR yielded a higher ΔP_1 in the mouse lung, suggesting an increase in airway resistance. The higher pressure used to overcome the elastic components (elastances) indicates a stiffer lung, while the larger ΔP_2 points towards a more inhomogeneous distribution of ventilation and/or a more prominent viscoelasticity. Such mechanical effects may be related to inflammation, as reflected by the increase in PMN cells in the lung parenchyma and the augmented area of alveolar collapse. Some reports have already related alterations in pulmonary tissue mechanics resulting from the inflammatory process. Other toxic substances such as snake venom and lipopolysaccharides can cause these effects and damage lung tissue as well (Faffe et al., 2000; Silveira et al., 2004).

ELISA could not detect the presence of MCYST-LR in the mice lungs. The data on the activity of protein phosphatases strengthen this result, since no inhibitory effect on PP1 and 2A was found. This would not be the case if most of the microcystin were bound to lung phosphatases. Even though, the hypothesis that the toxin reached the lung in very low concentrations cannot be discarded. However, the most probable explanation to these observations stems from the fact that the liver represents the target organ for microcystins, because of the ability of hepatocytes to uptake these toxins through bile acid transporters (Robinson et al., 1991; Carmichael, 1994). Besides, i.p. injection favors microcystin conveyance straight to the liver, since the toxin reaches initially the portal vein circulation, and, from there reaches the liver. In fact, liver analyses of these animals showed the presence of toxin, which affected protein phosphatases activity (unpublished data).

On the other hand, i.p. injection of microcystins can stimulate peritoneal macrophages to produce inflammatory mediators, such as tumor necrosis factor-alpha (TNF-α). This was observed by Nakano et al. (1991) after i.p. administration of MCYST-LR and toxic extracts of *M. aeruginosa* to mice. They also suggest that these macrophages could be producing interleukin-1 (IL-1) as well. Wagner and Roth (2000) stated that IL-1 is an important stimulator of PMN cells migration to the lung parenchyma. Hence, in our study, if MCYST-LR did not reach the lungs, it is possible that the inflammatory process was started by cytokines

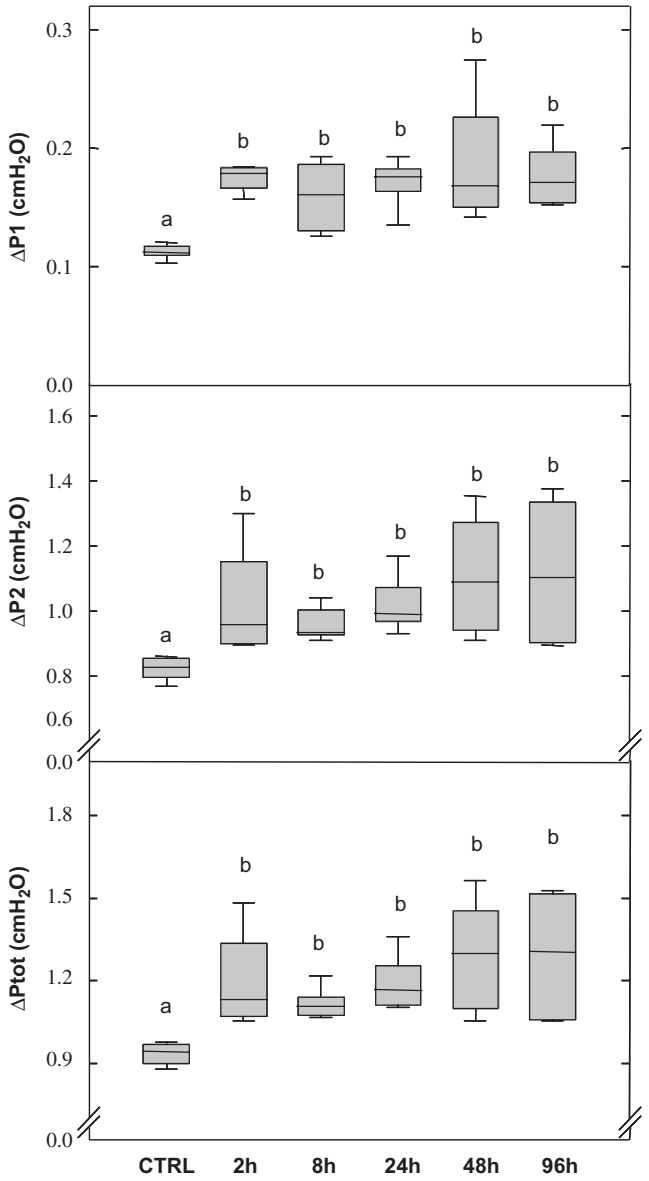

Fig. 3. Resistive mechanical parameters in mice. Box plot of six animals in each group (10–15 determinations per animal). Boxes show interquartile (25–75%) range, whiskers encompass range, and horizontal lines represent median values. ΔP_1, resistive pressure; ΔP_2, pressure dissipated to overcome viscoelastic/inhomogeneous mechanical components of the lung; ΔP_{tot}, total pressure spent against viscous and viscoelastic components; CTRL, animals that were injected intraperitoneally with saline solution (0.9% NaCl); CYANO, mice that received i.p. injection of microcystin-LR (40 μg/kg of body weight). Measurements were done after 2, 8, 24, 48 and 96 h after the injection. Different letters indicate significantly different values ($p<0.05$).

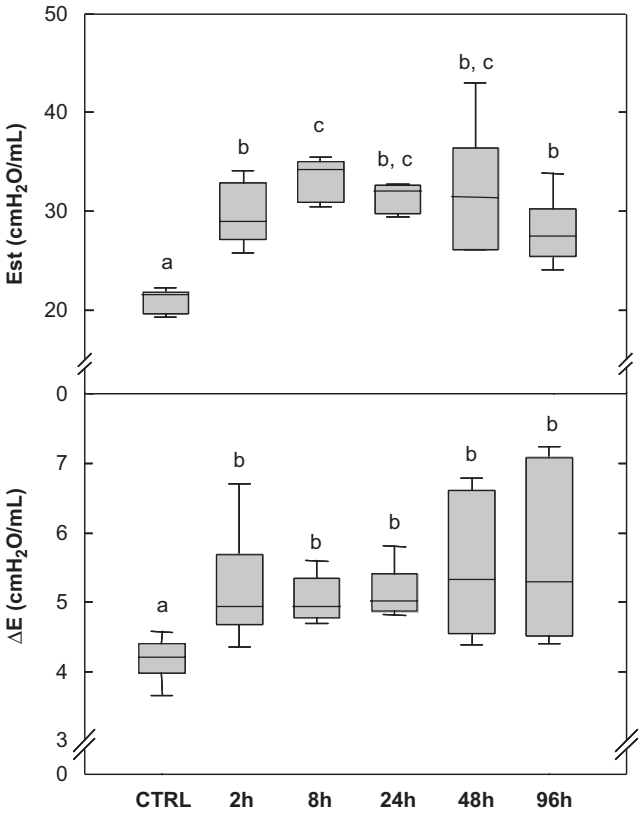

Fig. 4. Elastic mechanical parameters in mice. Box plot of six animals in each group (10–15 determinations per animal). Boxes show interquartile (25–75%) range, whiskers encompass range, and horizontal lines represent median values. E_{st}, static elastance; ΔE, difference between static and dynamic elastances; CTRL, animals that were injected intraperitoneally with saline solution (0.9% NaCl); CYANO, mice that received i.p. injection of microcystin-LR (40 μg/kg of body weight). Measurements were done after 2, 8, 24, 48 and 96 h after the injection. Different letters indicate significantly different values ($p<0.05$).

produced by peritoneal macrophages and carried by the blood stream. In fact, there are several reports on extrapulmonary lung injury which demonstrate lung involvement in a more distant systemic inflammatory response (Rocco and Zin, 2005; Menezes et al., 2005). Moreover, it can be hypothesized that a damaged liver can generate and release inflammatory mediators causing this secondary lung injury, especially since the pulmonary artery draws blood from the posterior vena cava, supplied by the hepatic portal vein. Nobre et al. (2003) could also see that macrophages stimulated by MCYST-LR release mediators capable to promote nephrotoxicity in isolated perfused rat kidney. They believe that phospholipase A2, TNF-α and other mediators appear to be involved in this renal toxic mechanism.

If some MCYST-LR did reach the lungs, it is possible that it has directly promoted the inflammatory response. Naseen et al. (1989) showed, in *in vitro* studies, that MCYST-LR stimulated alveolar macrophages to produce prostaglandins F2 and PGE2, as well as tromboxane B2 and arachidonic acid—all inflammatory mediators.

The inflammatory process can damage the lung tissue by means of reactive oxygen species (ROS) produced by activated defense cells, such as neutrophils, monocytes and macrophages (Klaassen, 1996). In our study, such phenomenon could explain the increase in the amount of alveolar collapse in MCYST-LR-injected mice, because damaged type II pneumocytes might not produce surfactant in adequate amounts.

The results allow us to conclude that a sub-lethal dose of i.p. injected MCYST-LR can generate an acute inflammatory process in mice lungs. Although the i.p. administration is not the most direct way to simulate the common contact of animals or humans with microcystins dissolved in water, it approximates the hemodialysis route of exposure, so it can be considered very useful in toxicological studies. Exposure of animals and humans to low concentrations of microcystins is much more frequent than lethal intoxication events. Therefore, knowledge of its effects on the diverse organs is certainly necessary.

Acknowledgments

We would like to express our gratitude to Mr. Antonio Carlos de Souza Quaresma and Veronica Cristina dos Santos for their skillful technical assistance.

We would also like to thank Professor Wayne W. Carmichael (Wright State University, OH, USA) for his kindness in providing the MCYST-LR standard, anti-MCYST-LR polyclonal antibodies and MCYST-HRP conjugate (for ELISA).

This work was supported by the Centers of Excellence Program (PRONEX-MCT and PRONEX-FAPERJ), the Brazilian Council for Scientific and Technological Development (CNPq), and the Carlos Chagas Filho Rio de Janeiro State Research Supporting Foundation (FAPERJ).

References

An, J., Carmichael, W.W., 1994. Use of a olorimetric protein phosphatase inhibition assay and enzyme linked immunosorbent assay for the study of microcystins and nodularins. Toxicon 32 (12), 1495–1507.

Azevedo, S.M.F.O., Carmichael, W.W., Jochimsen, E.M., Rinehart, K.L., Lau, S., Shaw, G.R., Eaglesham, G.K., 2002. Human intoxication by microcystins during renal dialysis treatment in Caruaru—Brazil. Toxicology 181, 441–446.

Bates, J.H., Rossi, A., Milic-Emili, J., 1985. Analysis of the behavior of the respiratory system with constant inspiratory flow. J. Appl. Physiol. 58, 1840–1848.

Bates, J.H.T., Ludwig, M.S., Sly, P.D., Brown, K.A., Martin, J.G., Fredberg, J.J., 1988. Interrupter resistance elucidated by alveolar pressure measurement in open-chest normal dogs. J. Appl. Physiol. 65, 408–414.

Botha, N., Venter, M.V., Downing, T.G., Shephard, E.G., Gehringer, M.M., 2004. The effect of intraperitoneally administered microcystin-LR on gastrointestinal tract of Balb/c mice. Toxicon 43, 251–254.

Carmichael, W.W., 1994. The toxins of cyanobacteria. Sci. Am. 270, 78–86.

Carmichael, W.W., An, J.S., 1999. Using an enzyme linked immunosorbent assay (ELISA) and a protein phosphatase inhibition assay (PPIA) for the detection of microcystins and nodularins. Nat. Toxins 7 (6), 377–385.

Carmichael, W.W., Azevedo, S.M.F.O., An, J., Molica, R.J.R., Jochimsen, E.M., Lau, S., Rinehart, K.L., Shaw, G.R., Eaglesham, G.K., 2001. Human fatalities from cyanobacteria: chemical and biological evidence for cyanotoxins. Environ. Health Perspect. 109, 663–668.

Chorus, I., Bartram, J. (Eds.), 1999. Toxic Cyanobacteria in Water—A Guide to Their Public Health Consequences, Monitoring and Management. E & FN Spon., London, 416pp.

Chu, F.S., Huang, X., Wei, R.D., 1990. Enzyme-linked immunosorbent assay for microcystins in blue-green algal blooms. J. Assoc. Anal. Chem. 7, 451–454.

Faffe, D.S., Seidl, V.R., Chagas, P.S.C., Moraes, V.L.G., Capelozzi, V.L., Rocco, P.R.M., Zin, W.A., 2000. Respiratory effects of lipopolysaccharide-induced inflammatory lung injury in mice. Eur. Respir. J. 15, 85–91.

Falconer, I.R., Smith, J.V., Jackson, A.R.B., Jones, A., Runnegar, M.T.C., 1988. Oral toxicity of a bloom of the cyanobacterium *Microcystis aeruginosa* administered to mice over periods up to 1 year. J. Toxicol. Environ. Health 24, 291–305.

Ferrão-Filho, A.S., Azevedo, S.M.F.O., 2002. Effects of unicellular and colonial forms of toxic *Microcystis aeruginosa* from laboratory cultures and natural populations on tropical cladocerans. Aquat. Ecol. 37, 23–35.

Francis, G., 1878. Poisonous Australian lake. Nature 18, 11–12.

Gundersen, H.J.G., Bendtsen, T.F., Korbo, L., Marcussen, N., Moller, A., Nielsen, K., Nyengaard, J.R., Pakkenberg, B., Sorensen, F.B., Vesterby, A., West, M.J., 1988. Some new, simple and efficient seterological methods and their use in pathological research and diagnosis. APMIS 96, 379–394.

Humpage, A.R., Hardy, S.J., Moore, E.J., Froscio, S.M., Falconer, I.R., 2000. Microcystins (cyanobacterial toxins) in drinking water enhance the growth of aberrant crypt foci in the mouse colon. J. Toxicol. Environ. Health 61, 155–165.

Ito, E., Kondo, F., Harada, K.-I., 2000. First report on the distribution of orally administered microcystin-lr in mouse tissue using an immunostaining method. Toxicon 38, 37–48.

Ito, E., Kondo, F., Harada, K.-I., 2001. Intratracheal administration of microcystin-LR and its distribution. Toxicon 39, 265–271.

Jochimsen, E.M., Carmichael, W.W., An, J.S., Cardo, D.M., Cookson, S.T., Holmes, C.E.M., Antunes, M.B.C., Melo-Filho, D.A., Lyra, T.M., Barreto, V.S.T., Azevedo, S.M.F.O., Jarvis, W.R., 1998. Liver failure and death after exposure to microcystins at a haemodialysis center in Brazil. New Engl. J. Med. 33, 873–878.

Klaassen, C.D., 1996. Cassarett and Doull's Toxicology: The Basic Science of Poisons, fifth ed. Health Professions Division, McGraw-Hill, 1211pp.

Kochi, T., Okubo, S., Zin, W.A., Milic-Emili, J., 1988. Flow and volume dependence of pulmonary mechanics in anesthetized cats. J. Appl. Physiol. 64, 441–450.

Menezes, S.L.S., Bozza, P.T., Neto, H.C.C.F., Laranjeira, A.P., Negri, E.M., Capelozzi, V.L., Zin, W.A., Rocco, P.R.M., 2005. Pulmonary and extrapulmonary acute lung injury: inflammatory and ultrastructural analyses. J. Appl. Physiol. 98, 1777–1783.

Moreno, I.M., Mate, A., Repetto, G., Vazquez, C.M., Camean, A.M., 2003. Influence of microcystin-LR on the activity of membrane enzymes in rat intestinal mucosa. J. Physiol. Biochem. 59 (4), 293–299.

Mortola, J.P., Noworaj, A., 1983. Two-sidearm tracheal cannula for respiratory airflow measurements in small animals. J. Appl. Physiol. 55, 250–253.

Nagase, T., Lei, M., Robatto, F.M., Eidelman, D.H., Ludwig, M.S., 1992. Tissue viscance during induced constriction in rabbit lung: morphological–physiological correlation. J. Appl. Physiol. 73, 1900–1907.

Nakano, Y., Shirai, M., Mori, N., Nakano, M., 1991. Neutralization of microcystin shock in mice by tumor necrosis factor alpha antiserum. Appl. Environ. Microbiol. 57, 327–330.

Naseen, S.M., Hines, H.B., Creasia, D.A., 1989. Effect of toxins on arachidonic acid metabolism in rat cultured pulmonary alveolar macrophages. Biochem. Inter. 19, 583–592.

Nobre, A.C.L., Coêlho, G.R., Coutinho, M.C.M., Silva, M.M.M., Angelim, E.V., Menezes, D.B., Fonteles, M.C., Monteiro, H.S.A., 2001. The role of phospholipase a_2 and cyclooxygenase in renal toxicity induced by microcystin-LR. Toxicon 39, 721–724.

Nobre, A.C.L., Martins, A.M.C., Havt, A., Benevides, C., Lima, A.A.M., Fonteles, M.C., Monteiro, H.S.A., 2003. Renal effects of supernatant from rat peritoneal macrophages activated by microcystins-LR: role protein mediators. Toxicon 41, 377–381.

Pflugmacher, S., 2002. Possible allelopathic effects of cyanotoxins, with reference to microcystin-LR, in aquatic ecosystems. Environ. Toxicol. 17, 407–413.

Picanço, M.R., Soares, R.M., Cagido, V.R., Azevedo, S.M.F.O., Rocco, P.R.M., Zin, W.A., 2004. Toxicity of a cyanobacterial extract containing microcystins to mouse lungs. Braz. J. Med. Biol. Res. 37 (8), 1225–1229.

Robinson, N.A., Matson, C.F., Pace, J.G., 1991. Association of microcystin-LR and its biotranformation product with a hepatic-cytosolic protein. J. Biochem. Toxicol. 6, 171–180.

Rocco, P.R.M., Zin, W.A., 2005. Pulmonary and extrapulmonary acute respiratory distress syndrome: are they different? Curr. Opin. Crit. Care 11, 10–17.

Runnegar, M.T., Kong, S., Berndt, N., 1993. Protein phosphatase inhibition and in vivo hepatotoxicity of microcystins. Am. J. Physiol. 265 (Gastrointst. Liver Physiol., v.28), g224–g230.

Sahin, A., Tencalla, F.G., Dietrich, D.R., Mez, K., Naegeli, H., 1995. Enzymatic analysis of liver samples from rainbow trout for diagnosis of blue-green algae-induced toxicosis. Am. J. Vet. Res. 56 (8), 1110–1115.

Shenolikar, S., Ingebritsen, T.S., 1984. Protein (serine and threonine) phosphatases. Methods Enzymol. 107, 103–129.

Silveira, K.S.O., Boechem, N.T., Nascimento, S.M., Murakami, V.L.B., Barboza, A.P.B., Melo, P.A., Castro, P., Moraes, V.L.G., Rocco, P.R.M., Zin, W.A., 2004. Pulmonary mechanics and lung histology in acute lung injury induced by *Bothrops jararaca* venom. Respir. Physiol. Neurobiol. 139, 167–177.

Similowski, T., Levy, P., Corbeil, C., Albala, M., Pariente, R., Derenne, J.P., Bates, J.H.T., Jonson, B., Milic-Emili, J., 1989. Viscoelastic behavior of lung and chest wall in dogs determined by flow interruption. J. Appl. Physiol. 67, 2219–2229.

Slatkin, D.N., Stoner, R.D., Adams, W.H., Kycia, J.H., Siegelman, H.W., 1983. Atypical pulmonary thrombosis caused by a toxic cyanobacterial peptide. Science 220, 1383–1385.

Soares, R.M., Yuan, M., Servaites, J.C., Delgado, A., Magalhães, V.F., Hilborn, E.D., Carmichael, W.W., Azevedo, S.M.F.O., 2006. Sublethal exposure from microcystins to renal insufficiency patients in Rio de Janeiro, Brazil. Environ. Toxicol. 21 (2), 95–103.

Turner, P.C., Gammie, A.J., Hollinrake, K., Codd, G.A., 1990. Pneumonia associated with cyanobacteria. Br. Med. J. 300, 1400–1414.

Wagner, J.G., Roth, R.A., 2000. Neutrophil migration mechanisms, with an emphasis on the pulmonary vasculature. Pharmacol. Rev. 52 (3), 349–374.